

Double-Pomeron-Exchange Contribution to the Reaction $pp \rightarrow pp\pi^+\pi^-$ at 205 GeV/c

M. Derrick, B. Musgrave, P. Schreiner, and H. Yuta
 Argonne National Laboratory, Argonne, Illinois 60439
 (Received 10 October 1973)

The reaction $pp \rightarrow pp\pi^+\pi^-$ at 205 GeV/c is analyzed in terms of the rapidities of the secondary particles to measure the contribution of the double-Pomeron exchange process. Using a sample of 191 events, we estimate the maximum possible contribution for this process to be $44 \mu\text{b}$ for the region of πp effective mass greater than 2.0 GeV in a total cross section of $680 \pm 140 \mu\text{b}$.

Many of the features of high-energy reactions observed in the CERN intersecting storage rings and with the bubble chamber at the National Accelerator Laboratory (NAL) have been understood in terms of multiperipheral ideas.¹ The nature of the exchange particles has not been explicitly studied except that Pomeron exchange is thought to be responsible for the diffractively produced events. In one of the simplest multiperipheral models,² multi-Pomeron exchange processes with nonzero couplings would lead to divergence problems in the cross section, so it is important to search for evidence of multi-Pomeron exchange.

We have looked for double-Pomeron exchange (DPE) in the reaction

$$pp \rightarrow p\pi^+\pi^-p \quad (1)$$

at 205 GeV/c which would occur via the diagram of Fig. 1(a). This diagram, with a single pion loop, is perhaps the simplest case where one might see evidence for DPE. Reaction (1) has been extensively studied for momenta up to 28 GeV/c,³ and several attempts have been made to evaluate the DPE contribution.^{4,5} However, at low energies such a contribution in the central rapidity region is essentially masked by the pro-

nounced $p\pi^+\pi^-$ low-mass enhancements resulting from diagrams such as 1(b) and 1(c), so that the earlier estimates were not conclusive. The present experiment has the advantage that at our high energy a much larger range of rapidity space is available to the secondaries, which reduces the degree of overlap between the diffractive and any DPE contributions in the central rapidity region.

The data were obtained from 50 000 pictures taken with the 30-in. hydrogen bubble chamber exposed to a 205-GeV/c proton beam at NAL. The results reported here are based on 191 $pp\pi^+\pi^-$ events selected by kinematic fitting from 1191 successfully reconstructed four-prong events in a 36-cm-long fiducial volume. A detailed discussion of the fitting and event selection is contained in Derrick *et al.*⁶ We measure the cross section for Reaction (1) to be $680 \pm 140 \mu\text{b}$, where the error quoted includes our estimate of the possible contamination.

Figures 2(a)–2(d) show the $p\pi^+\pi^-$, $p\pi^+$, $p\pi^-$, and $\pi^+\pi^-$ mass distributions, respectively, and summarize the prominent features of Reaction (1). The $p\pi^+\pi^-$ low-mass enhancement, which results from diffractive excitation of the proton, and pronounced $p\pi^+$ and $p\pi^-$ low-mass peaks dominate the reaction in a way similar to what is seen at lower energies. The $\pi^+\pi^-$ mass distribution in Fig. 1(d) shows that the di-pion mass tends to be small with most events falling below the ρ mass. There is no evidence for strong production of either $\rho(765)$ or $f(1260)$, in qualitative agreement with results at 24 GeV/c.⁵

To isolate the DPE contribution, one can impose cuts on the various subenergies to restrict the rapidities of the secondaries. Figures 3(a)–3(c) show the longitudinal center-of-mass (c.m.) rapidity distributions of the pions and protons for the fitted events. There is good overall forward-backward symmetry in each case, demonstrating that our fitted sample is not strongly

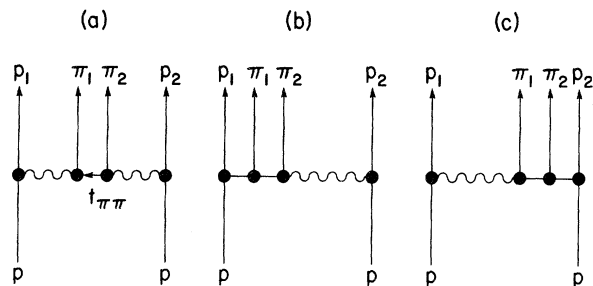


FIG. 1. Feynman diagrams representing (a) double-Pomeron exchange and (b), (c) diffractive production of the $p\pi^+\pi^-$ system.

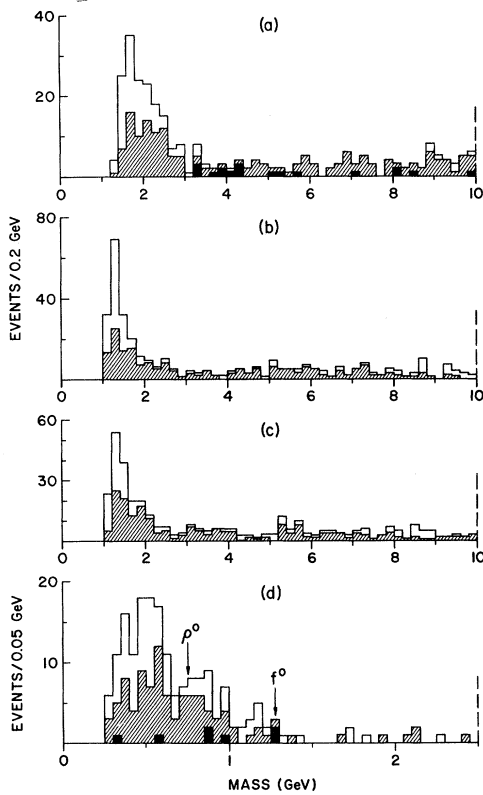


FIG. 2. The effective-mass distribution for (a) the $p\pi^+\pi^-$, (b) the $p\pi^+$, (c) the $p\pi^-$, and (d) the $\pi^+\pi^-$ systems. The hatched events correspond to those where both protons are at the ends of the rapidity chain; the blackened events also have the $p\pi$ effective masses greater than 2 GeV.

affected by any bias or contamination. Over all, the low-mass $p\pi\pi$ system is associated with a single proton in the opposite hemisphere with an average gap from this leading proton to the $p\pi\pi$ system of ~ 5 units. The $p\pi\pi$ system has a dispersion of ± 1 units of rapidity, and this combined with the $p\pi\pi$ and $\pi\pi$ mass distributions of Fig. 2 shows that most of the $\pi^+\pi^-$ pairs are emitted as a result of diffractive excitation of either the beam or the target proton. Since we expect the pion pairs from the DPE process to have a large rapidity gap from both protons, we first impose a restriction that the longitudinal c.m. rapidities of both the π^+ and π^- lie between the two proton rapidities as implied by the diagram of Fig. 1(a). Events selected in this way are shown hatched in Fig. 2.

Figure 3(d) shows the longitudinal c.m. rapidity ($Y_{\pi\pi}$) distribution for the $\pi^+\pi^-$ system considered as a single particle. The hatched area again corresponds to the rapidity selection de-

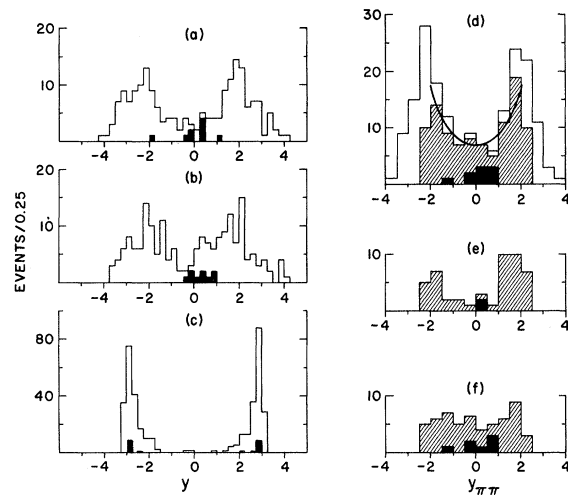


FIG. 3. The c.m. longitudinal rapidity distribution for (a) the π^+ , (b) the π^- , and (c) the proton from Reaction (1); and the c.m. rapidity distribution for the $\pi^+\pi^-$ system (d) for all the $\pi\pi$ mass range, (e) for the $\pi\pi$ mass less than 0.6 GeV, and (f) for the $\pi\pi$ mass greater than 0.6 GeV. The hatched events correspond to those where both protons are at the ends of the ordered rapidity chain; the shaded events also have the $p\pi$ effective masses greater than 2 GeV.

scribed above. The clear double-peaked structure is attributed to the $p\pi^+\pi^-$ low-mass enhancement observed in Fig. 2(a). The double-Pomeron contribution is expected to be most easily seen in the central region where the distribution is flat within our statistics. This is true both for the total sample as well as for the hatched events. However, since the tails from the diffractive process also populate the central region, any estimate of the DPE contribution can be strongly influenced by the parametrization adopted for the diffractive process.

To isolate a possible DPE contribution, we simply define as diffractive those events having any one of the four possible $p\pi$ masses less than 2.0 GeV. This leaves the nine events⁷ shown in black on Figs. 2(a), 2(d), and 3. Most of the nine events are in the central region of rapidity, i.e., $|Y_{\pi\pi}| < 1.0$. Effectively, these mass cuts remove all the events having $p\pi^+\pi^-$ mass less than 3 GeV as well as the low-mass $p\pi^+$ and $p\pi^-$ enhancements. The remainder contains the possible DPE contribution plus other contributions such as single diffraction in the region of $p\pi$ mass greater than 2 GeV, and these nine events correspond to a cross section of $44 \pm 15 \mu\text{b}$.⁸

The y distributions of the individual π and p tracks of these nine events are shown blackened

in Fig. 3. The proton tracks are limited to the large- y region. An examination of the x ($x = 2p_{||}^*/\sqrt{s}$) distribution shows that all events have both protons with $|x| \geq 0.75$ and five of the nine have both protons in the region $|x| \geq 0.9$ where Pomeron exchange dominates.

However, we find that the events in the central rapidity region mainly come from those with $\pi^+\pi^-$ mass greater than 0.6 GeV, whereas we expect the DPE process to be dominated by a low-mass s -wave $\pi\pi$ system. This is best shown by the $Y_{\pi\pi}$ distributions of Figs. 3(e) and 3(f), where the $\pi^+\pi^-$ mass is selected to be less than 0.6 GeV and greater than 0.6 GeV, respectively. As indicated by the hatching, events in both plots satisfy the rapidity ordering previously discussed. We note that with the restriction of $M_{\pi\pi} < 0.6$ GeV, we obtain a cross section of $9 \mu\text{b}$ based on two events.

The diagrams of Fig. 1 assuming a fixed $\pi\pi$ mass suggests a $Y_{\pi\pi}$ distribution of the form⁹

$$\frac{dN}{dY_{\pi\pi}} = 2A^2 \cosh^2(\delta Y_{\pi\pi}) + 2AB \cosh(\delta Y_{\pi\pi}) + B^2,$$

where A and B are the parameters to characterize the diffraction and the double-Pomeron processes, respectively, and δ is the difference between the intercepts of the Pomeron and the f Regge trajectories, taken to be 0.5. We have fitted the hatched distribution in Fig. 3(d) by this form. In the fit, we only consider $|Y_{\pi\pi}| < 2.0$ where the above formula should be appropriate to our data. We find that the DPE parameter B is consistent with being zero.¹⁰ The best-fitting curve is shown in Fig. 3(d). We note that the nonzero value in the central rapidity region comes from the diffractive component of $2A^2$.

A naive calculation of the DPE contribution based on the Amati-Bertocchi-Fubini-Stanghellini-Tonin (ABFST) model,² without introducing any form factor, gives¹¹ a cross section of $70 \mu\text{b}$ for the region of the $p\pi$ mass greater than 2 GeV and $|t_{\pi\pi}| < 0.5 \text{ GeV}^2$. Here $t_{\pi\pi}$ is the square of the momentum transfer between the two pions as shown in Fig. 1(a). For the same $p\pi$ mass and $t_{\pi\pi}$ selection, we measured a cross section of $24 \pm 11 \mu\text{b}$ which is substantially less than that calculated.¹²

In conclusion, we see no evidence for a double-Pomeron-exchange contribution to the $p\pi^+\pi^-p$ final state and measure the maximum possible

DPE contribution of $44 \pm 15 \mu\text{b}$ for the region of the $p\pi$ mass greater than 2 GeV. Compared to a naive ABFST calculation of the DPE calculation of the DPE contribution in a restricted $p\pi$ mass and $t_{\pi\pi}$ region, our data give a cross section which is smaller by a factor of about 3.

We acknowledge the effort of the NAL staff for providing this exposure, and of the Argonne National Laboratory film scanning group. We are also grateful to D. Sivers, D. Snider, S. Pinsky, B. Webber, and R. Shankar for stimulating discussions.

*Work supported by the U. S. Atomic Energy Commission.

¹M. Jacob, CERN Report No. TH 1683-CERN, 1973 (unpublished).

²G. F. Chew *et al.*, Phys. Rev. D **2**, 765 (1970); L. Bertocchi *et al.*, Nuovo Cimento **25**, 626 (1962); D. Amati *et al.*, Nuovo Cimento **26**, 6 (1962).

³CERN Report No. CERN/HERA 70-2, 1970 (unpublished).

⁴J. G. Rushbrook, in *Proceedings of the Third International Colloquium on Multiparticle Reactions, Zakopane, Poland, 1972*, edited by O. Czyzewski and L. Michejda (Nuclear Energy Information Center of the Polish Government Commissioner, Warsaw, Poland, 1972), p. 441.

⁵U. Idschok *et al.*, Nucl. Phys. **B53**, 282 (1973).

⁶M. Derrick *et al.*, "The Reaction $pp \rightarrow pp\pi^+\pi^-$ at 205 GeV/c" (to be published).

⁷D. M. Chew and R. Shankar, Lawrence Berkeley Laboratory Physics Report No. TG-205, 1973 (unpublished). If we remove events having either $p_1\pi_1$ or $p_2\pi_2$ mass less than 2 GeV, where p_i and π_i ($i=1,2$), respectively, denote the proton and pion of Fig. 1(a), we obtain an extra two events. Both of them have a smaller $p\pi\pi$ mass than 3 GeV and a large $|Y_{\pi\pi}|$ of order of 2.

⁸A similar result has been obtained using the reaction $\pi^-p \rightarrow \pi^-\pi^+\pi^-p$ at 205 GeV/c: D. M. Chew *et al.*, Lawrence Berkeley Laboratory Report No. 2106, 1973 (unpublished).

⁹We thank S. Pinsky for providing the formula.

¹⁰Without restrictions on the parameter B , we obtain a negative value of B from the fit. Since the parameter B is physically expected to be positive, the best fit is obtained by setting $B=0$ and gives $A=1.89 \pm 0.06$.

¹¹We thank D. Snider for calculating the cross section.

¹²A recent calculation by R. Shankar using a form factor at the π - π -Pomeron vertices of Fig. 1(a) [Lawrence Berkeley Report No. 2068, 1973 (unpublished)] gives a double-Pomeron cross section of $31.3 \mu\text{b}$ compared to our measured $44 \pm 15 \mu\text{b}$.